Ab initio carbon capture in open-site metal–organic frameworks

Allison L. Dzubak[1†], Li-Chiang Lin[2†], Jihan Kim[3], Joseph A. Swisher[2,3], Roberta Poloni[2,4], Sergey N. Maximoff[2], Berend Smit[2,3]* and Laura Gagliardi[1]*

During the formation of metal–organic frameworks (MOFs), metal centres can coordinate with the intended organic linkers, but also with solvent molecules. In this case, subsequent activation by removal of the solvent molecules creates unsaturated 'open' metal sites known to have a strong affinity for CO_2 molecules, but their interactions are still poorly understood. Common force fields typically underestimate by as much as two orders of magnitude the adsorption of CO_2 in open-site Mg-MOF-74, which has emerged as a promising MOF for CO_2 capture. Here we present a systematic procedure to generate force fields using high-level quantum chemical calculations. Monte Carlo simulations based on an *ab initio* force field generated for CO_2 in Mg-MOF-74 shed some light on the interpretation of thermodynamic data from flue gas in this material. The force field describes accurately the chemistry of the open metal sites, and is transferable to other structures. This approach may serve in molecular simulations in general and in the study of fluid–solid interactions.

Most energy scenarios project a significant increase in the role of renewable energy sources[1]. These scenarios also predict an even higher increase in our energy needs. As a consequence, although the relative consumption of fossil fuels will be decreasing, in absolute terms we will continue to burn more coal. In such a scenario, carbon capture and sequestration will be one of the only viable technologies to mitigate CO_2 emissions[1,2]. At present the cost associated with the capture of CO_2 from flue gas is one of the bottlenecks in the large-scale deployment of this technology. Of particular concern is that the efficiency of a coal-fired power plant decreases by as much as 30–40% (ref. 3) because of the energy required to separate and compress CO_2. The aim of decreasing this parasitic load has motivated the search for novel materials[4,5].

A promising class of materials is metal–organic frameworks (MOFs)[4,6]. MOFs are crystalline materials that consist of metal centres connected by organic linkers. These materials have an extremely large internal surface area and, compared to other common adsorbents, promise very specific customization of their chemistry. By changing the metal and the linker, one can in principle generate many millions of possible materials. In practice, however, we can synthesize only a very small fraction of these materials, and it is important to develop a theoretical method that supports the experimental efforts to identify an ideal MOF for carbon capture. A key aspect is the ability to predict the properties of a MOF before the material is synthesized. At present it is possible to carry out accurate quantum chemical calculations on these types of systems[7]. State-of-the-art density functional theory (DFT) calculations provide important insights into the energetics and siting of CO_2 at zero Kelvin[7]. The separation of flue gas, however, requires thermodynamic information (for example, adsorption isotherms) at flue-gas conditions (40 °C and 1 atm). This type of information can be obtained from molecular simulation using classical force fields.

For some classes of MOFs these predictions still pose significant difficulties, namely for MOFs with unsaturated—referred to as 'open'—metal sites[8–15]. These materials crystallize in such a way that both linkers and solvent molecules coordinate to the metal centres. The stability of the materials allows the removal of the solvent, which creates an open metal site. This site has a very high affinity for CO_2, which makes the material very promising for carbon capture. Often, reasonable predictions on the ability of a material to adsorb CO_2 can be made using existing generic force fields[16–18]. However, for these materials Krishna and van Baten observed that, exactly at the conditions that are important for flue-gas capture, the universal force field (UFF)[19] fails to describe correctly the adsorption of CO_2 (ref. 18). The reason is that an open metal site imposes a chemical environment very different from those considered in the development of these force fields.[12]

Ideally, we would use state-of-the-art quantum chemical calculations to evaluate the energy for each state point of a grand canonical Monte Carlo (GCMC) simulation to compute the adsorption isotherm. However, such calculations would require millions of years of central processing unit time. In this work, we developed a methodology to obtain accurate force fields (parameters that describe the potential energy of a system) from quantum calculations to predict correctly the adsorption isotherms of CO_2 and N_2 on MOFs with open metal sites. Our approach is based on the non-empirical model potential (NEMO) methodology[20,21], which decomposes the total electronic interaction energy obtained from quantum chemical calculations into the various contributions (electrostatic, repulsive, dispersion and so on). The force-field expression closely matches the functional form of the NEMO decomposition, which allows us to fit accurately the parameters of the force field to reproduce the quantum calculations. We developed a strategy to obtain the interaction for each atom type of the MOF with CO_2 (or N_2).

The UFF[19] or Dreiding[22] force field are used frequently to describe the interaction of gas molecules with the atoms of the MOF[16,17,23]. In these force fields, the energy of non-covalently bonded atoms is described by a Lennard-Jones potential plus Coulomb interactions. As these force fields are employed for

[1]Department of Chemistry and Supercomputing Institute, University of Minnesota, 207 Pleasant Street SE, Minneapolis, Minnesota 55455-0431, USA, [2]Department of Chemical and Biomolecular Engineering and Chemistry, University of California, Berkeley, Berkeley, California 94720-1462, USA, [3]Materials Science Division, Lawrence Berkeley National Laboratory, Berkeley, California 94720, USA, [4]Molecular Foundry, Lawrence Berkeley National Laboratory, Berkeley, California 94720, USA, [†]These authors contributed equally to this work. *e-mail: Berend-Smit@berkeley.edu; gagliard@umn.edu

many different systems, the parameters should give a reasonable description of the interaction of CO_2 with Mg in many different chemical environments. Our quantum calculations, however, show that owing to the open metal site of Mg-MOF-74, CO_2 (and N_2) can get closer to the magnesium centre than is predicted by the UFF. The aim of this work is to develop a systematic methodology to obtain force fields from quantum chemical calculations that describe correctly the interaction of the guest gas with the open metal site. To our knowledge, no existing force field is able to describe this interaction correctly.

Our aim is to determine a complete isotherm at flue-gas conditions, which requires taking into account ensemble averages that involve billions of different configurations. Therefore, in the development of a force field we have to ensure that a large number of different configurations for the system are described in a reasonable way, and not just the minimum energy configuration, which is usually the focus of a quantum chemical calculation.

Results and discussion

We employed quantum chemical calculations based on a NEMO decomposition of the total energy of the MOF–CO_2 and MOF–N_2 systems. Energies obtained with Møller-Plesset second-order perturbation theory (MP2) are decomposed into the corresponding electrostatic, repulsive and attractive contributions, which include dispersion, exchange interactions and polarization (see Supplementary Information, part 1, for details). The importance of this decomposition is that we can fit the corresponding terms in our force field separately.

Force-field parameter determination. In our force field, the electrostatic interactions are described by charges estimated using the LoProp scheme[24]. With this approach it is possible to partition molecular properties, such as multipole moments and polarizabilities, into atomic and interatomic contributions. The method requires a subdivision of the atomic basis set into occupied and virtual basis functions for each atom in the molecular system. Initial tests showed that the repulsive interactions could not be described accurately with a Lennard-Jones potential. (The Lennard-Jones potential is a mathematically simple model that approximates the interaction between a pair of neutral atoms or molecules with $1/r^6$ and $1/r^{12}$ terms, where r is the distance between the two atoms or molecules). A modified Buckingham potential was used in addition to the Coulomb interaction:

$$u^{\text{rep}}(r) = \begin{cases} \infty & r < r_{\min} \\ A\exp(-Br) & r > r_{\min} \end{cases} \qquad (1)$$

which can be fitted very accurately. For the attractive part, we used, in addition to the conventional r^6 term, an r^5 term to obtain a better representation of the decomposed energies:

$$u^{\text{att}}(r) = \frac{C}{r^5} + \frac{D}{r^6} \qquad (2)$$

To determine the parameters of this force field, we used the following procedure. First, we generated sets of configurations
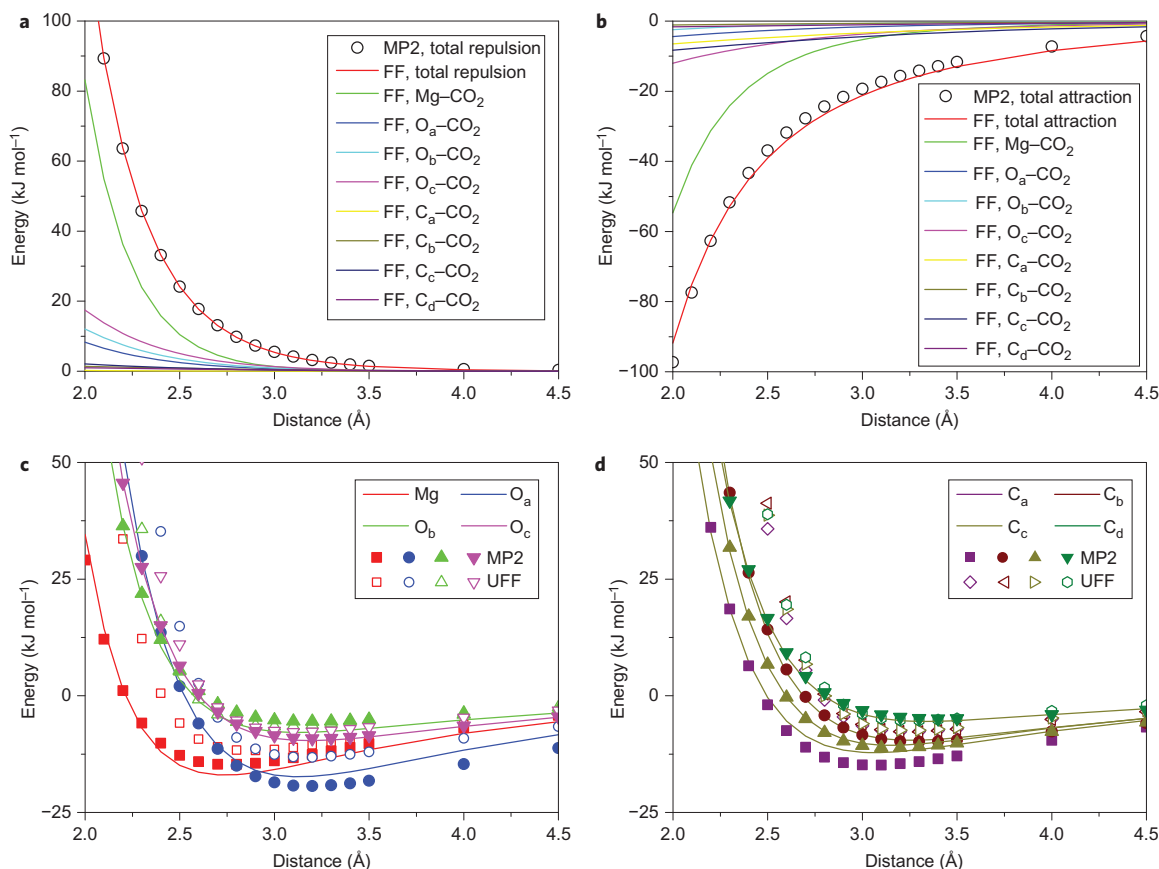

Figure 1 | Interaction energy comparison of force fields with decomposed MP2 and UFF. a,b, NEMO decomposition of the MP2 energies on the Mg path into repulsive (**a**) and attractive (**b**) interactions. The black circles are the MP2 results and the solid lines are the fitted force fields for the various atoms. The red line gives the contribution of Mg. **c,d,** Comparison of the MP2 repulsive and attractive energies (filled symbols) for the eight different paths with the force-field results (lines). Mg and O paths (**c**) and C paths (**d**) are compared with the predictions from UFF (open symbols).
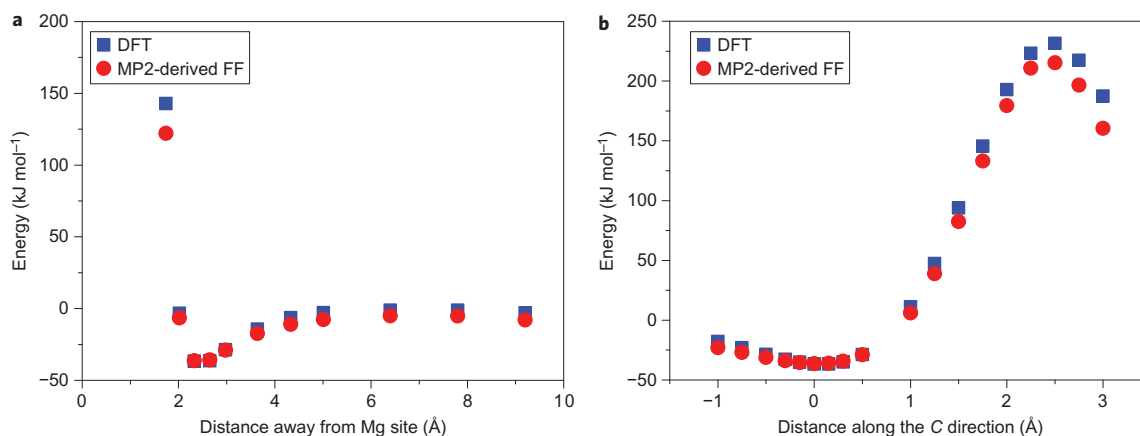
Figure 2 | Interaction energy comparison of force field with periodic DFT. a,b, The MOF–CO_2 interaction energy is plotted along two different paths that cross the minimum energy configuration of CO_2 in Mg-MOF-74: CO_2 approaching the open metal site from the centre of the pore (**a**) and CO_2 approaching the open metal site in the *C*-direction (**b**). Blue curves are DFT calculations that include van der Waals interactions and red curves are obtained from our force field. Both paths are computed in the periodic system.

organized into paths, with one path for each type of atom in the framework, that is, Mg, O_a, O_b, O_c, C_a, C_b, C_c and C_d in Mg-MOF-74 (Supplementary Fig. S1). Along each path, CO_2 (or N_2) approaches a specific atom type in such a way that for each configuration on this path the MP2 energy mainly represents the interaction of CO_2 (or N_2) with this particular atom type. These energies should thus contribute the most to the fitting of the parameters of the force field for this particular atom type. As it is infeasible to carry out MP2 calculations for the full periodic MOF, we defined for each atom type (and corresponding path) a finite cluster of atoms within the MOF that should represent the electronic environment of this atom type in the MOF. The size of the cluster was set such that the interaction of CO_2 (or N_2) with this atom type mimics the interaction in the full MOF.

The decomposition in electrostatic, repulsive and attractive interactions for each path allowed us to fit this relatively large number of force-field parameters efficiently and accurately. This procedure was

Figure 3 | Comparison of the experimental and simulated isosteric heats of adsorptions as a function of loading. The loading is plotted as the number of CO_2 molecules per open metal site. For an ideal material, for which all metal sites are active, the molecular simulations (blue symbols) predict that one CO_2 binds to one open metal site. The black, green and olive symbols give the reported experimental data of Mason et al.[11], Dietzel et al.[10] and Simmons et al.[25], respectively. Red lines indicate the enhancement of the CO_2 heat of adsorption caused by cooperative effects and was predicted from the molecular simulations.

used to determine the interactions of the end atom of the guest molecules (O of CO_2) with the atoms of the MOF. We then performed Monte Carlo simulations, which showed that the oxygen atoms dominate the interactions with the framework. The interactions with the interior atom of the guest molecules (that is, C of CO_2) were too weak to be included in this process.

For each of these paths, we selected a portion of the Mg-MOF-74 framework that was sufficiently large to represent accurately the chemical environment of the targeted atom. The size of the cluster was chosen in a compromise between accuracy and computational cost, with the size of the basis set as a constraint. The clusters corresponding to the eight paths and the details of the MP2 calculations are described in the Supplementary Information, parts 1, 10.

Figure 1a,b shows a typical outcome of the NEMO decomposition of the total MP2 energies into repulsive (Fig. 1a) and attractive (Fig. 1b) contributions for the Mg atom–CO_2 interaction, along with the fitted force fields. The electrostatic (charge–charge) contribution is identical to the leading term of the grouped-term NEMO decomposition, so no fitting is required. This figure illustrates that, indeed, the interaction of CO_2 with Mg dominates the total energy along this path. The repulsive interactions on this path are described accurately with our force field. As the attractive interaction contains many different contributions and the functional form of the attractive interaction in our model only approximates the corresponding MP2 interactions, the fit of the attractive part is less accurate than that of the repulsive part. Similar results were obtained for the other paths. Figure 1c,d shows that our force field can reproduce the total MP2 energies for all paths to within 1–2 kJ mol^{-1}.

To further validate our procedure, we compared the energies obtained from our force field with those obtained from DFT calculations on the fully periodic framework for two different paths. These DFT calculations include dispersive interactions as implemented in van der Waals density functional (vdW-DF), and the computed CO_2–MOF binding energies and geometries are similar to those reported by Valenzano et al.[7] (see Supplementary Information, part 2). Figure 2 shows that our results are in good agreement with the DFT results. It is important that the path shown in Fig. 2a includes the minimum energy configurations, a feature that is reproduced well by our force field. The detailed force fields for the interactions of CO_2 and N_2 with Mg-MOF-74 are reported in Supplementary Tables S4–S13.

It is instructive to compare our force field with that obtained by UFF. In Fig. 1c,d we compare the UFF predictions of the total
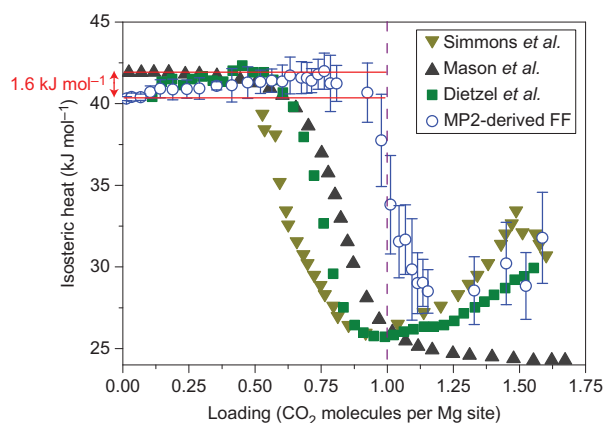
energies on the eight different paths. For the Mg path, we observe that the UFF does not allow the CO_2 molecule to approach the Mg atom as close as the MP2 calculations predict. As a consequence, the electrostatic and dispersive interactions are underestimated significantly. That we can incorporate these chemical differences in our force field is essential for a correct description of these systems; otherwise, it would not possible to reproduce the results of the quantum calculations.

Predictions from simulations that utilize the new force field. As a first test of our force field we computed the heat of adsorption and compared it with the experimental values obtained by Simmons et al.[25], Dietzel et al.[10] and Mason et al.[11] (Fig. 3). Our simulations reproduced quantitatively the observed dependence of the heat of adsorption as a function of loading. We predicted an inflection at exactly one CO_2 molecule per Mg, but the experiments show this inflection at slightly lower loadings (~0.8 CO_2 molecule per Mg). In our simulation we assumed a perfect crystalline material in which every Mg atom was activated—as all Mg atoms are equivalent, one would expect this inflection to occur at exactly one CO_2 molecule per Mg. These observations support the conclusion of Dietzel et al.[10], according to which, not all Mg sites are accessible in the real system. Our simulations, in agreement with the experimental data of both Dietzel et al.[10] and Simmons et al.[25], showed an increase in the heat of adsorption as a function of the loading. Mason et al.[11], however, did not report

such an increase. They obtained the heat of adsorption from a fitting procedure to a dual-site Langmuir isotherm. This procedure imposes a monotonic decrease of the heat of adsorption as a function of loading. In this study we computed the experimental heat of adsorption directly from our simulations[26], and hence our results are independent of the interpretation of the isotherms.

In Fig. 4 we compare the predicted adsorption isotherms with the experimental isotherms for CO_2 and N_2 in Mg-MOF-74 (refs 10, 11, 25, 27–31). We obtained excellent agreement with experimental data, and the agreement is best when we take into account that not all the Mg sites are accessible in the experiments. Comparison with the simulation using the UFF illustrates the significant improvement in predictions made by our force field. In the Henry regime, the conventional force field underestimates the adsorption by as much as two orders of magnitude. An interesting observation is that we were not able to describe the simulated (and experimental) adsorption isotherms for CO_2 with a dual-site Langmuir isotherm (see Fig. 5). Langmuir isotherms assume that each adsorption site is independent. The heat of adsorption data already show that CO_2–CO_2 interactions cannot be ignored for the CO_2 binding to the Mg sites and, because of these interactions, it becomes easier to add another CO_2 molecule in the MOF. If we have a loading of approximately one CO_2 per six Mg, we observe a significant collective effect that makes it easier to add an additional CO_2 molecule adjacent to those already adsorbed.
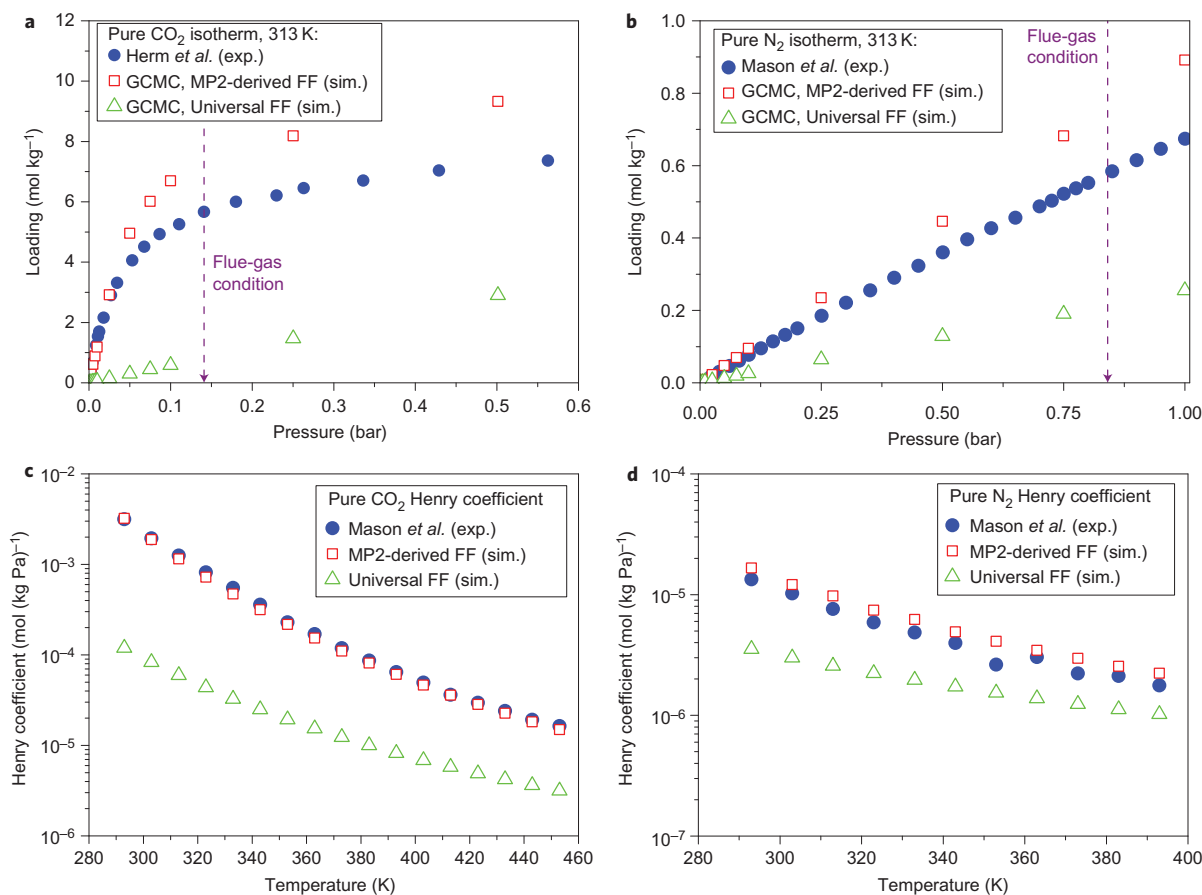

Figure 4 | Comparison of simulated and experimental adsorption isotherms and Henry coefficients. a,b, Experimental (exp.) and predicted (sim.) adsorption isotherms are shown for CO_2 (**a**) and N_2 (**b**) in Mg-MOF-74. The experimental data of Herm et al.[30] or Mason et al.[11] are shown by the filled blue circles. The open symbols are the simulation results: the green symbols are the results of using the UFF and the red symbols are from the present force field. At low pressure the adsorption is linear in pressure (the proportionality coefficient is defined as the Henry coefficient). **c,d**, The Henry coefficients are shown as a function of the temperature for CO_2 (**c**) and N_2 (**d**).
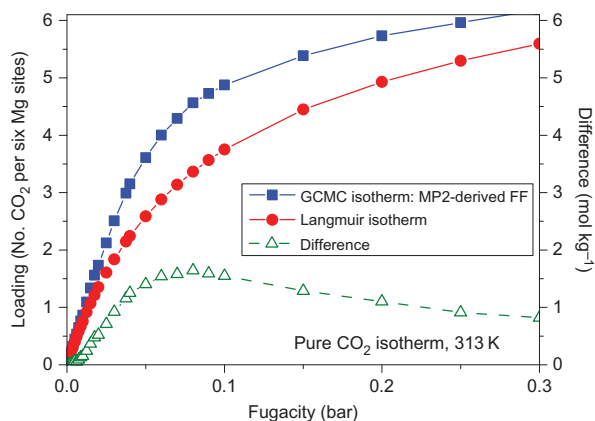
Figure 5 | Enhancement of the adsorption of CO$_2$ as a function of loading. In this figure we compare a Langmuir isotherm (red) with the results from GCMC simulations (blue). The parameters of the Langmuir isotherm are obtained from the Henry coefficient from the GCMC simulations and the maximum loading, which is set to one CO$_2$ per Mg site. The difference between these curves (green) indicates the enhancement induced by the presence of other CO$_2$ molecules.

Figure 5 shows that these relatively small energies (1.6 kJ mol^{-1}), provided by the CO$_2$–CO$_2$ interactions, essentially enhance the uptake of CO$_2$ by up to 15% at the condition of carbon capture. This suggests that in the design of a carbon-capture material one would also want to optimize these collective effects inside the material. In addition, therefore, we performed simulations to predict the adsorption isotherms for a CO$_2$–N$_2$ mixture (see Supplementary Information, part 8). To the best of our knowledge, mixture adsorption isotherms have not been measured for this system, yet they are essential to determine the performance of a material for carbon capture.

At this point it is instructive to compare our approach with the multi-Langmuir approach that Sauer *et al.*[32] developed. In the multi-Langmuir method, the MP2 energies at the binding sites are used directly to estimate the corresponding adsorption coefficient (or Henry coefficient) of the different adsorption sites and hence the use of force fields is avoided. The multi-Langmuir approach relies on the assumption that the isotherms can be described with a Langmuir equation and so a few well-defined binding sites dominate adsorption. As for the adsorption of CO$_2$ in Mg-MOF-74, the use of a force field is essential to capture the enhancement at low loading and to describe correctly the adsorption at high loading.

Transferability
We now discuss the transferability of our approach. Recently, McDonald *et al.*[15] synthesized Mg$_2$(dobpdc) (in which dobpdc is 4,4′-dioxido-3,3′-biphenyldicarboxylate), a material similar to MOF-74, but with an extended linker. As this linker contains atom types similar to those in MOF-74, we can compute the isotherms for Mg$_2$(dobpdc) using the force field derived for Mg-MOF-74. Figure 6a shows that the predicted isotherm is in good agreement with the experimental data that McDonald *et al.*[15] reported. We also investigated the effect of changing the metal in MOF-74. In Supplementary Information, part 6, we show that the Zn-MOF-74 isotherm can be computed by recalculating the force field for the CO$_2$ metal interactions, but keeping all other interactions the same as those in Mg-MOF-74. This result is further confirmation that our approach is transferable. In Fig. 6b we compare the predicted isotherms for Zn-MOF-74 with the corresponding isotherm for Mg-MOF-74. Unfortunately, Zn-MOF-74
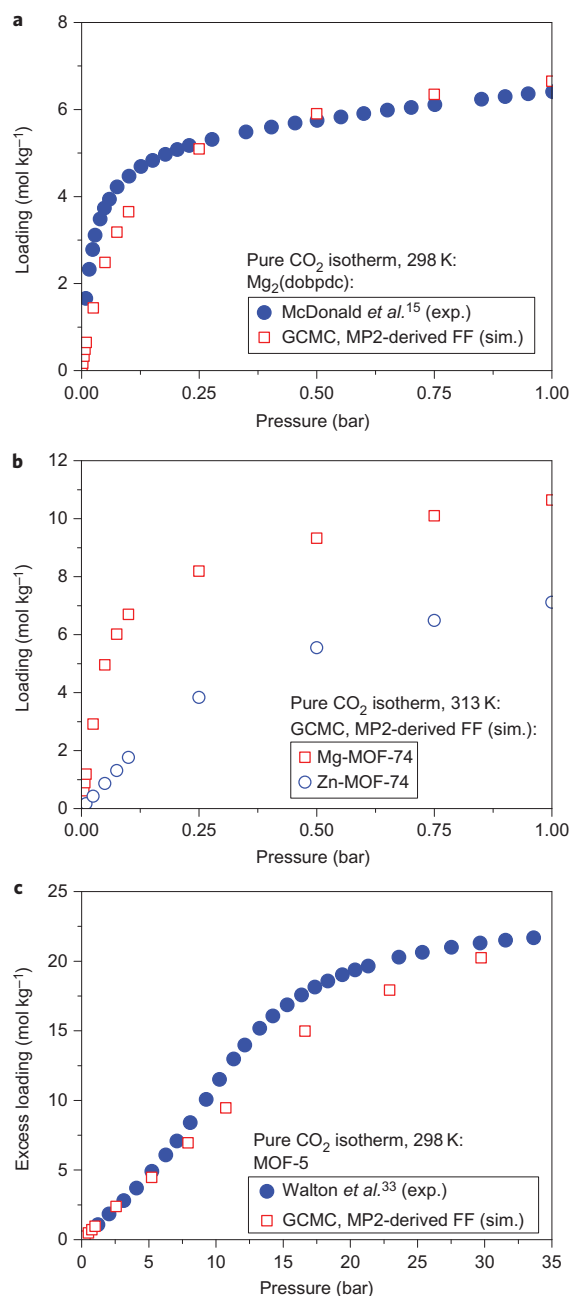

Figure 6 | Adsorption isotherms of CO$_2$ in additional frameworks. **a–c**, Transferability of the methodology was studied in three additional frameworks: Mg$_2$(dobpdc), which is a material with an extended linker using the same atom types as in the Mg-MOF-74 material (**a**); Mg-MOF-74 and Zn-MOF-74, in which we tested the transferability of our force field for the metal sites by replacing the Mg by the Zn force field, but keeping the force field for the atoms in the linker identical (**b**); MOF-5, a material that does not have open metal sites (**c**). Closed and open symbols represent the experimental and simulation adsorption isotherms, respectively.

is much more difficult to activate and hence there are no definitive experimental results to compare our predictions against. Finally, we employed our approach to study CO$_2$ in MOF-5, which does not have open metal sites. Figure 6c shows that the CO$_2$ simulated isotherm is in excellent agreement with the experimental one that Walton *et al.*[33] reported. This set of results confirms that our methodology is applicable to different types of structures.

Conclusions

In summary, a novel methodology that yields accurate force fields for CO_2 and N_2 in an open-site MOF from high-level quantum chemical calculations was developed. These force fields take into account the subtle changes in the chemical environment induced by the presence of open metal sites in MOFs. Our method allows us to reproduce the experimental adsorption isotherms for both CO_2 and N_2 in Mg-MOF-74 and to predict the mixture isotherms at flue-gas conditions. We also showed that our methodology is transferable to systems that contain different metals, linkers and topologies. The same approach will be used to predict properties of open-site MOFs that have not yet been synthesized.

Methods

MP2 calculations. In this work, we used MP2 to describe interactions of CO_2 and N_2 with MOF sites. MP2 is adequate for the treatment of electron correlation in cases where strong correlations are not present. In the Mg-MOF-74, we defined eight representative clusters of the MOF to compute interactions with the guest, each cluster chosen to best represent the atom type to be parameterized (excluding H atom types). Within each cluster, the basis functions were chosen such that a larger contraction was used for the guest atoms, the atom type being approached in the MOF, and its nearest neighbours. A smaller contraction was used for all atoms farther away. The choice of clusters, basis function contractions and discussion of convergence are given in the Supplementary Information, parts 1, 10. The interaction energies were determined by the supermolecular approach, counterpoise corrected for the basis-set superposition error[34]. All calculations were performed using the MOLCAS software version 7.6 (ref. 35). Resolution of the identity and Cholesky decomposition techniques was employed to treat the two electron integrals[36–38]. The Douglas–Kroll–Hess Hamiltonian[39] was used in conjunction with basis functions of the atomic natural orbital relativistic correlation consistent (ANO-RCC)[40,41] type.

DFT calculations. The optimized crystal structure was obtained from DFT as implemented in the Vienna *ab initio* simulation package (VASP)[42,43], employing the Perdew–Burke–Ernzerhof gradient-corrected exchange-correlation functional. Interaction energies were computed using the vdW-DF (refs 44,45) as implemented in SIESTA (refs 46,47). Basis-set superposition errors were counterpoise corrected. More details about our DFT calculations are given in the Supplementary Information.

SIESTA calculations used variationally optimized double-Z polarized basis sets that imply the presence of *d*-orbitals for C, N and O. Non-local, norm-conserving fully separable Trouiller–Martins pseudopotentials were used. C ($2s2p$), O ($2s2p$) and Mg ($2s2p3s$) electrons were included explicitly in the valence. Real-space integrals were performed on a mesh with a 300 Ry cutoff.

VASP calculations use projector-augmented wave potentials to describe the interaction between core and valence electrons. C ($2s2p$), O ($2s2p$), Mg ($3s3p$) and Zn ($4p3d$) valence electrons were included explicitly in the valence. A plane-waves kinetic energy cutoff of 500 eV was used and the integration over the irreducible Brillouin zone was carried out over a $2 \times 2 \times 8$ Monkhorst-Pack grid. Atomic positions were relaxed until the forces were lower than 0.02 eV Å^{-1}.

NEMO decomposition and force-field parameterization. Using the MP2 interaction energies as a reference, the NEMO decomposition[21] was used to partition the energy into repulsion, polarization, dispersion and electrostatic components (functional form given in the Supplementary Information, part 1.5) for all clusters and paths. The electrostatic moments to second order and dipole–dipole polarizabilities were obtained using the LoProp method[24] based on the MP2 densities[48]. The terms were then grouped into repulsive, attractive and electrostatic terms, in which the charge–charge interactions and repulsions remained constant, and the polarization, dispersion and effects of dipoles and quadrupoles were grouped into attraction terms (see equations (1) and (2)), for which the parameters were then fitted by atom pairs. For this mapping procedure, in which the decomposed energies were parameterized separately, only the parameters for the interaction between the target-atom type and the guest molecule were adjusted to reproduce the NEMO-decomposed energy. This mapping was carried out in two phases. We first took all atoms of a particular element and minimized the error over all paths for that element simultaneously. This adjustment was done moving outwards from the metal, and started over again interactively until convergence. For the second phase, we optimized the force-field parameters for each atom type individually with an ordering based on its relative contribution to the total energy. The ratio of the energy between the target-atom type and the guest molecule to the total energy was computed, and the paths were taken in sequence from the highest to the lowest ratio. This procedure was repeated until all the parameters were converged (Supplementary Information, part 3).

GCMC simulations. Adsorption (pure and mixture) isotherms for CO_2 and N_2 in Mg-MOF-74 were predicted using the GCMC technique, in which a constant chemical potential (fugacity), volume and temperature were imposed[49]. The heat of adsorption was calculated directly using the procedure developed by Vuong and Monson[26]. The energies of guest–framework interactions were computed using the potential model described above and guest–guest interactions were described using the transferable potentials for phase equilibria force fields[50]. Electrostatic energy was computed using the Ewald summation technique. Short-range interactions were cut off and shifted to zero at a distance of 12.8 Å, and the simulation box was extended by at least twice this distance in all orthogonal directions. No tail correction was used. To accelerate the calculation of molecule–framework interaction energies, the short-range part of the interaction was stored in a precomputed grid with a spacing of 0.10 Å and linearly interpolated between grid points. Trajectories were equilibrated for at least 20 million configurations before averages were taken over a further four million configurations.

References

1. Pacala, S. & Socolow, R. Stabilization wedges: solving the climate problem for the next 50 years with current technologies. *Science* **305**, 968–972 (2004).
2. Metz, B., Davidson, O., deConinck, H., Loos, M. & Meyer, L. *IPCC Special Report on Carbon Dioxide Capture and Storage*. Intergovernmental Panel on Climate Change (Cambridge Univ. Press, 2005).
3. Ramezan, M., Skone, T. J., ya Nsakala, N. & Liljedahl, G. N. *Carbon Dioxide Capture from Existing Coal-Fired Power Plants*. Report No. DOE/NETL-401/110907 (National Energy Technology Laboratory, US Department of Energy, 2007).
4. D'Alessandro, D. M., Smit, B. & Long, J. R. Carbon dioxide capture: prospects for new materials. *Angew. Chem. Int. Ed.* **49**, 6058–6082 (2010).
5. Lin, L-C. *et al. In silico* screening of carbon-capture materials. *Nat. Mater.* **11**, 633–641 (2012).
6. Sumida, K. *et al.* Carbon dioxide capture in metal–organic frameworks. *Chem. Rev.* **112**, 724–781 (2012).
7. Valenzano, L., Civalleri, B., Sillar, K. & Sauer, J. Heats of adsorption of CO and CO_2 in metal–organic frameworks: quantum mechanical study of CPO-27-M (M = Mg, Ni, Zn). *J. Phys. Chem. C* **115**, 21777–21784 (2011).
8. Chui, S. S-Y., Lo, S. M-F., Charmant, J. P. H., Orpen, A. G. & Williams, I. D. A chemically functionalizable nanoporous material. *Science* **283**, 1148–1150 (1999).
9. Millward, A. R. & Yaghi, O. M. Metal–organic frameworks with exceptionally high capacity for storage of carbon dioxide at room temperature. *J. Am. Chem. Soc.* **127**, 17998–17999 (2005).
10. Dietzel, P. D. C., Besikiotis, V. & Blom, R. Application of metal–organic frameworks with coordinatively unsaturated metal sites in storage and separation of methane and carbon dioxide. *J. Mater. Chem.* **19**, 7362–7370 (2009).
11. Mason, J. A., Sumida, K., Herm, Z. R., Krishna, R. & Long, J. R. Evaluating metal–organic frameworks for post-combustion carbon dioxide capture via temperature swing adsorption. *Energy Environ. Sci.* **4**, 3030–3040 (2011).
12. Grajciar, L. S., Bludský, O. & Nachtigall, P. Water adsorption on coordinatively unsaturated sites in CuBTC MOF. *J. Phys. Chem. Lett.* **1**, 3354–3359 (2010).
13. Getman, R. B., Bae, Y-S., Wilmer, C. E. & Snurr, R. Q. Review and analysis of molecular simulations of methane, hydrogen, and acetylene storage in metal–organic frameworks. *Chem. Rev.* **112**, 703–723 (2012).
14. Wu, H., Zhou, W. & Yildirim, T. High-capacity methane storage in metal–organic frameworks M(2)(dhtp): the important role of open metal sites. *J. Am. Chem. Soc.* **131**, 4995–5000 (2009).
15. McDonald, T. M. *et al.* Capture of carbon dioxide from air and flue gas in the alkylamine-appended metal–organic framework mmen-Mg_2(dobpdc). *J. Am. Chem. Soc.* **134**, 7056–7065 (2012).
16. Yazaydin, A. O. *et al.* Screening of metal–organic frameworks for carbon dioxide capture from flue gas using a combined experimental and modeling approach. *J. Am. Chem. Soc.* **131**, 18198 (2009).
17. Liu, B. & Smit, B. Comparative molecular simulation study of CO_2/N_2 and CH_2/N_2 separation in zeolites and metal–organic frameworks. *Langmuir* **25**, 5918–5926 (2009).
18. Krishna, R. & van Baten, J. M. *In silico* screening of metal–organic frameworks in separation applications. *Phys. Chem. Chem. Phys.* **13**, 10593–10616 (2011).
19. Rappe, A. K., Casewit, C. J., Colwell, K. S., Goddard, W. A. & Skiff, W. M. UFF, a full periodic table force field for molecular mechanics and molecular dynamics simulations. *J. Am. Chem. Soc.* **114**, 10024–10035 (1992).
20. Hagberg, D., Karlstrom, G., Roos, B. O. & Gagliardi, L. The coordination of uranyl in water: a combined quantum chemical and molecular simulation study. *J. Am. Chem. Soc.* **127**, 14250–14256 (2005).
21. Engkvist, O., Astrand, P. O. & Karlstrom, G. Accurate intermolecular potentials obtained from molecular wave functions: bridging the gap between quantum chemistry and molecular simulations. *Chem. Rev.* **100**, 4087–4108 (2000).
22. Mayo, S. L., Olafson, B. D. & Goddard, W. A. Dreiding – a generic force-field for molecular simulations. *J. Phys. Chem.* **94**, 8897–8909 (1990).
23. Krishna, R. & van Baten, J. M. Investigating the potential of MgMOF-74 membranes for CO_2 capture. *J. Membr. Sci.* **377**, 249–260 (2011).

24. Gagliardi, L., Lindh, R. & Karlstrom, G. Local properties of quantum chemical systems: the LoProp approach. *J. Chem. Phys.* **121,** 4494–4500 (2004).

25. Simmons, J. M., Wu, H., Zhou, W. & Yildirim, T. Carbon capture in metal–organic frameworks—a comparative study. *Energy Environ. Sci.* **4,** 2177–2185, (2011).

26. Vuong, T. & Monson, P. A. Monte Carlo simulation studies of heats of adsorption in heterogeneous solids. *Langmuir* **12,** 5425–5432 (1996).

27. Liu, J. *et al*. Stability effects on CO_2 adsorption for the DOBDC series of metal–organic frameworks. *Langmuir* **27,** 11451–11456 (2011).

28. Bao, Z. B., Yu, L. A., Ren, Q. L., Lu, X. Y. & Deng, S. G. Adsorption of CO_2 and CH_4 on a magnesium-based metal organic framework. *J. Colloid Interface Sci.* **353,** 549–556 (2011).

29. Caskey, S. R., Wong-Foy, A. G. & Matzger, A. J. Dramatic tuning of carbon dioxide uptake via metal substitution in a coordination polymer with cylindrical pores. *J. Am. Chem. Soc.* **130,** 10870 (2008).

30. Herm, Z. R., Swisher, J. A., Smit, B., Krishna, R. & Long, J. R. Metal–organic frameworks as adsorbents for hydrogen purification and precombustion carbon dioxide capture. *J. Am. Chem. Soc.* **133,** 5664–5667 (2011).

31. Kizzie, A. C., Wong-Foy, A. G. & Matzger, A. J. Effect of humidity on the performance of microporous coordination polymers as adsorbents for CO_2 capture. *Langmuir* **27,** 6368–6373 (2011).

32. Sillar, K., Hofmann, A. & Sauer, J. *Ab initio* study of hydrogen adsorption in MOF-5. *J. Am. Chem. Soc.* **131,** 4143–4150 (2009).

33. Walton, K. S. *et al*. Understanding inflections and steps in carbon dioxide adsorption isotherms in metal–organic frameworks. *J. Am. Chem. Soc.* **130,** 406–407 (2008).

34. Boys, S. F. & Bernardi, F. Calculation of small molecular interactions by differences of separate total energies – some procedures with reduced errors. *Mol. Phys.* **19,** 553–566 (1970).

35. Karlstrom, G. *et al*. MOLCAS: a program package for computational chemistry. *Comp. Mater. Sci.* **28,** 222–239 (2003).

36. Aquilante, F., Pedersen, T. B. & Lindh, R. Low-cost evaluation of the exchange Fock matrix from Cholesky and density fitting representations of the electron repulsion integrals. *J. Chem. Phys.* **126,** 194106 (2007).

37. Aquilante, F., Malmqvist, P. A., Pedersen, T. B., Ghosh, A. & Roos, B. O. Cholesky decomposition-based multiconfiguration second-order perturbation theory (CD-CASPT2): application to the spin-state energetics of Co-III(diiminato)(NPh). *J. Chem. Theory Comput.* **4,** 694–702 (2008).

38. Aquilante, F. *et al*. Accurate *ab initio* density fitting for multiconfigurational self-consistent field methods. *J. Chem. Phys.* **129,** 024113 (2008).

39. Hess, B. A. Relativistic electronic-structure calculations employing a 2-component no-pair formalism with external-field projection operators. *Phys. Rev. A* **33,** 3742–3748 (1986).

40. Roos, B. O., Lindh, R., Malmqvist, P. A., Veryazov, V. & Widmark, P. O. Main group atoms and dimers studied with a new relativistic ANO basis set. *J. Phys. Chem. A* **108,** 2851–2858 (2004).

41. Roos, B. O., Lindh, R., Malmqvist, P. A., Veryazov, V. & Widmark, P. O. New relativistic ANO basis sets for transition metal atoms. *J. Phys. Chem. A* **109,** 6575–6579 (2005).

42. Kresse, G. & Furthmuller, J. Efficiency of *ab-initio* total energy calculations for metals and semiconductors using a plane-wave basis set. *Comp. Mater. Sci.* **6,** 15–50 (1996).

43. Kresse, G. & Furthmuller, J. Efficient iterative schemes for *ab initio* total-energy calculations using a plane-wave basis set. *Phys. Rev. B* **54,** 11169–11186 (1996).

44. Lee, K., Murray, E. D., Kong, L. Z., Lundqvist, B. I. & Langreth, D. C. Higher-accuracy van der Waals density functional. *Phys. Rev. B* **82,** 081101 (2010).

45. Poloni, R., Smit, B. & Neaton, J. B. CO_2 capture by metal–organic frameworks with van der Waals density functionals. *J. Phys. Chem. A* **116,** 4957–4964 (2012).

46. Soler, J. M. *et al*. The SIESTA method for *ab initio* order-N materials simulation. *J. Phys. Condens. Matter* **14,** 2745 (2002).

47. Román-Peréz, G. & Soler, J. M. Efficient implementation of a van der Waals density functional: application to double-wall carbon nanotubes. *Phys. Rev. Lett.* **103,** 096102 (2009).

48. Holt, A., Bostrom, J., Karlstrom, G. & Lindh, R. A NEMO potential that includes the dipole–quadrupole and quadrupole–quadrupole polarizability. *J. Comput. Chem.* **31,** 1583–1591 (2010).

49. Frenkel, D. & Smit, B. *Understanding Molecular Simulations: from Algorithms to Applications* 2nd edn (Academic Press, 2002).

50. Potoff, J. J. & Siepmann, J. I. Vapor–liquid equilibria of mixtures containing alkanes, carbon dioxide, and nitrogen. *AIChE J.* **47,** 1676–1682 (2001).

Author contributions

A.L.D. performed the cluster calculations at the MP2 level and the NEMO decomposition of the interaction energies, R.P. performed the periodic DFT calculations, L-C.L., J.A.S. and J.K. performed the molecular simulations, S.N.M. provided some of the optimized MOF structures, A.L.D. and L-C.L. optimized the force field and B.S. and L.G. conceived the research. A.L.D., L-C.L., B.S. and L.G. co-wrote the manuscript and all the authors discussed the results and commented on the manuscript.

Additional information

Supplementary information is available in the online version of the paper. Reprints and permission information is available online at http://www.nature.com/reprints. Correspondence and requests for materials should be addressed to B.S. and L.G.

Competing financial interests

The authors declare no competing financial interests.